

RESEARCH ARTICLE

# The Characteristics and Regulatory Mechanisms of Superoxide Generation from eNOS Reductase Domain

Hu Peng<sup>1,2‡</sup>, Yugang Zhuang<sup>1,2‡</sup>, Yuanzhuo Chen<sup>1</sup>, Alicia N. Rizzo<sup>2</sup>, Weiguo Chen<sup>1,2\*</sup>

**1** Department of Emergency Medicine, Shanghai Tenth People's Hospital, Tongji University, Shanghai, China, **2** Division of Pulmonary, Critical Care, Sleep and Allergy, Department of Medicine, University of Illinois College of Medicine, Chicago, Illinois, United States of America

‡ These authors are joint first authors on this work.

\* [weiguo@uic.edu](mailto:weiguo@uic.edu)



**OPEN ACCESS**

**Citation:** Peng H, Zhuang Y, Chen Y, Rizzo AN, Chen W (2015) The Characteristics and Regulatory Mechanisms of Superoxide Generation from eNOS Reductase Domain. PLoS ONE 10(10): e0140365. doi:10.1371/journal.pone.0140365

**Editor:** Jian Fu, University of Kentucky, UNITED STATES

**Received:** July 24, 2015

**Accepted:** September 24, 2015

**Published:** October 14, 2015

**Copyright:** © 2015 Peng et al. This is an open access article distributed under the terms of the [Creative Commons Attribution License](https://creativecommons.org/licenses/by/4.0/), which permits unrestricted use, distribution, and reproduction in any medium, provided the original author and source are credited.

**Data Availability Statement:** All relevant data are within the paper.

**Funding:** The authors received no specific funding for this work.

**Competing Interests:** The authors have declared that no competing interests exist.

**Abbreviations:** BH<sub>4</sub>, Tetrahydrobiopterin; CaM, Calmodulin; DPI, Diphenyleneiodonium; DEPMPO, 5-diethoxyphosphoryl-5-methyl-1-pyrroline-*N*-oxide; eNOS, Endothelial nitric oxide synthase; eNOS RD, eNOS reductase domain; EPR, Electron paramagnetic resonance spectroscopy; FPLC, Fast

## Abstract

In addition to superoxide (O<sub>2</sub><sup>•-</sup>) generation from nitric oxide synthase (NOS) oxygenase domain, a new O<sub>2</sub><sup>•-</sup> generation site has been identified in the reductase domain of inducible NOS (iNOS) and neuronal NOS (nNOS). Cysteine S-glutathionylation in eNOS reductase domain also induces O<sub>2</sub><sup>•-</sup> generation from eNOS reductase domain. However, the characteristics and regulatory mechanism of the O<sub>2</sub><sup>•-</sup> generation from NOS reductase domain remain unclear. We cloned and purified the wild type bovine eNOS (WT eNOS), a mutant of Serine 1179 replaced with aspartic acid eNOS (S1179D eNOS), which mimics the negative charge caused by phosphorylation and truncated eNOS reductase domain (eNOS RD). Both WT eNOS and S1179D eNOS generated significant amount of O<sub>2</sub><sup>•-</sup> in the absence of BH<sub>4</sub> and L-arginine. The capacity of O<sub>2</sub><sup>•-</sup> generation from S1179D eNOS was significantly higher than that of WT eNOS (1.74:1). O<sub>2</sub><sup>•-</sup> generation from both WT eNOS and S1179D eNOS were not completely inhibited by 100nM tetrahydrobiopterin (BH<sub>4</sub>). This BH<sub>4</sub> uninhibited O<sub>2</sub><sup>•-</sup> generation from eNOS was blocked by 10mM flavoprotein inhibitor, diphenyleneiodonium (DPI). Purified eNOS reductase domain protein confirmed that this BH<sub>4</sub> uninhibited O<sub>2</sub><sup>•-</sup> generation originates at the FMN or FAD/NADPH binding site of eNOS reductase domain. DEPMPO-OOH adduct EPR signals and NADPH consumptions analyses showed that O<sub>2</sub><sup>•-</sup> generation from eNOS reductase domain was regulated by Serine 1179 phosphorylation and DPI, but not by L-arginine, BH<sub>4</sub> or calmodulin (CaM). In addition to the heme center of eNOS oxygenase domain, we confirmed another O<sub>2</sub><sup>•-</sup> generation site in the eNOS reductase domain and characterized its regulatory properties.

## Introduction

Endothelial nitric oxide synthase (eNOS, type III) is an important enzyme that is involved in a variety of fundamental functions such as cardiovascular tension regulation, proliferation of vascular smooth muscle cells, leukocyte adhesion and platelet aggregation [1–2]. The eNOS

Performance Liquid Chromatography;  $O_2^{\cdot-}$ , Superoxide; WT eNOS, Wild type eNOS; S1179D eNOS, Serine1179 aspartate eNOS mutant; NADPH, Nicotinamide adenine dinucleotide phosphate.

gene undergoes co-translational *N*-myristoylation and post-translational cysteine palmitoylation in the nuclear unit and Golgi, respectively [3–4]. Endothelial NOS (eNOS, type III) contains two functionally independent domains: an N-terminal oxygenase domain and a C-terminal reductase domain. In the eNOS oxygenase domain, there are sites that bind  $BH_4$  and L-arginine and convert L-arginine into L-citrulline, generating nitric oxide (NO). In the eNOS reductase domain, there are FMN and FAD/NADPH binding sequence and they are structurally and functionally similar with NADPH-cytochrome P-450 reductase. Between the oxygenase and reductase domains, there is an amino acid sequence binds to calmodulin (CaM). This region is necessary for maintaining the eNOS dimer structure and normal function.

Early in vitro studies demonstrated that all three kinds of NOS produced superoxide in L-arginine and  $BH_4$ -depleted condition [5–7]. Functional studies showed that superoxide ( $O_2^{\cdot-}$ ) formation from eNOS occurred primarily at the heme center of its oxygenase domain. This  $O_2^{\cdot-}$  synthesis from eNOS requires  $Ca^{2+}$ /CaM and is primarily regulated by  $BH_4$  rather than L-arginine[8]. The eNOS reductase domain contains 684 amino acids and there are two major subdomains: a FAD/NADPH binding sequence (758–1004), which generates the electrons and delivers them to the heme center of oxygenase domain of another monomer; two FMN binding sequences (from 522 to 705), which connect with the CaM binding sequence[9]. Glutamine 894, a reductase domain amino acid, polymorphisms changed eNOS response to L-arginine and further affected eNOS activity[10]. Recent study showed that S-glutathionylation of cysteines in eNOS reductase domain reversibly decreased eNOS activity and increased  $O_2^{\cdot-}$  generation. However, whether these cysteines glutathionylation-mediated  $O_2^{\cdot-}$  generation has not yet been fully investigated[11]. Additionally, a iNOS reductase domain subcloning study demonstrated that the FAD/NADPH and FMN binding sequence was another superoxide generation site in iNOS [12]. As all three isoforms of NOSs have FMN and FAD/NADPH binding sequence in reductase domains, it would be interesting to determine the  $O_2^{\cdot-}$  generation location and regulatory properties in eNOS reductase domain.

eNOS activity is regulated by cofactors as well as several critical amino acid modifications [13]. For example, the phosphorylation target of Akt is bovine Serine 1179 (Serine 1177 of human eNOS). Serine 1179 phosphorylation results in enhancement of eNOS activity and increased sensitivity to  $Ca^{2+}$  and CaM. Mutation of S1179 to aspartic acid (S1179D), which mimics the negative charge caused by phosphorylation, also increases eNOS activity [14–15]. Additionally, cytochrome C reduction studies demonstrate enhanced electron flux through the reductase domain of S1179D bovine eNOS compared to wild type eNOS [16]. Early in vitro studies demonstrated that heat shock protein 90 (HSP90), and not Serine 1179 phosphorylation, modulates  $O_2^{\cdot-}$  generation in endothelial cells using DMPO spin trapping [17]. However, recent studies indicate that  $O_2^{\cdot-}$  production in EC is regulated by eNOS Serine 1179 phosphorylation through two independent pathways: a direct pathway and an indirect pathways [18–21].

In this study, we utilized a stable spin trap probe (DEPMPO) with EPR to investigate whether the eNOS reductase domain has the potential to generate superoxide. We also aimed to determine if the classic eNOS cofactors ( $BH_4$ , L-arginine and  $Ca^{2+}$ /CaM) and Serine 1179 phosphorylation affect this  $O_2^{\cdot-}$  generation capability. Our results indicate that there is a  $O_2^{\cdot-}$  generation center in the FMN and FAD/NADPH binding site of the eNOS reductase domain. The  $O_2^{\cdot-}$  generation from the eNOS reductase domain is not affected by  $BH_4$ , L-arginine or  $Ca^{2+}$ /CaM. However, it is regulated by Serine 1179 phosphorylation and by flavoprotein inhibition.

## Materials and Methods

### Materials

Calcium chloride ( $\text{Ca}^{2+}$ ) and Calmodulin (CaM), >95% pure, were purchased from Sigma Chemical (St. Louis, MO). 2',5'-ADP-Sepharose 4B was the product of Amersham Pharmacia Biotech (Piscataway, NJ). L-[ $^{14}\text{C}$ ]arginine was from NEN (Boston, MA). NADPH, tetrahydrobiopterin,  $\text{N}^{\text{G}}$ -nitro-L-arginine methyl ester (L-NAME), diphenyleneiodonium (DPI) and other reagents were purchased from Sigma unless otherwise indicated. Both bovine WT eNOS pcDNA3 and S1179D eNOS pcDNA3 plasmids were purchased from [www.addgene.com](http://www.addgene.com).

### eNOS Purification

Both bovine WT eNOS and S1179D eNOS pcDNA 3 plasmid were used as templates and performed PCR. The forward primer was: 5' - CGGAATTCAACATGGGCAACTTGAAGAGTGTGGCCAG-3' and the backward primer is 5' -GCTCTAGATCATCAGGGGCCGGGGTGTCTGG-3'. The bovine eNOS reductase domain (521–1205) PCR forward primer was: 5' -CGGAATTC AACAAAGCAACCATCCTGTACG-3' and the backward primer is: 5' -GCTCTAGATCA TCAGGGGCCGGGGTGTCTGG-3' (start codon and stop codon was underlined). The PCR products were digested with EcoRI and XbaI and the product was subcloned into pCW plasmid [7, 22–23]. The resulting pCW plasmid was transformed into E.Coli (BL21) and cultured overnight. After harvesting the E.Coli by centrifugation, the bacteria pellet was homogenized in buffer A, which contains 50 mM Tris-HCl, pH 7.6, 0.1 mM EDTA, 150mM NaCl, 0.1mM DTT, 10% glycerol and protease inhibitor cocktail solution (Sigma). After being centrifuged (16,000 x g, 10 min) at 4°C, the supernatant was applied to a 2',5'-ADP-Sepharose 4B column pre-equilibrated in buffer A. The column was extensively washed with buffer A containing 600 mM NaCl and Tris-HCl buffer (50 mM, pH 7.6). The protein was then eluted with 5 mM AMP in 50 mM Tris-HCl (pH 7.6). The eluate was washed and concentrated using Centricon-100 (Amicon) concentrators. Further purification was performed using FPLC. The final purified WT and S1179D eNOS proteins were isolated from the fractions which had high absorption at 280nm and 408nm. Protein content of the preparations was assayed with the Bradford reagent (Bio-Rad) using bovine serum albumin as standard. The purity of eNOS was determined by SDS-PAGE and visualized with Coomassie brilliant blue (R-250, Bio-Rad) staining. The purified eNOS preparations exhibited one prominent band on gels with a molecular mass of 135 kDa. Purified eNOS samples were stored in 50 mM Tris-HCl (pH 7.6) buffer with 10% glycerol at -80°C.

### L-[ $^{14}\text{C}$ ]arginine to L-[ $^{14}\text{C}$ ]citrulline Conversion Assay

eNOS-catalyzed conversion of L-[ $^{14}\text{C}$ ]arginine to L-[ $^{14}\text{C}$ ]citrulline was monitored in a total volume of 200  $\mu\text{l}$  of buffer containing 50 mM Tris-HCl, pH 7.6, 2  $\mu\text{M}$  L-[ $^{14}\text{C}$ ]arginine, 0.5 mM NADPH, 0.5 mM  $\text{Ca}^{2+}$ , 10  $\mu\text{g}/\text{ml}$  calmodulin, 10  $\mu\text{M}$   $\text{BH}_4$ , and 10  $\mu\text{g}/\text{ml}$  purified eNOS. After five minutes incubation at 37°C, the reaction was terminated by adding 3 ml of ice-cold stop buffer (20 mM Hepes, pH 5.5, 2 mM EDTA, 2 mM EGTA). L-[ $^{14}\text{C}$ ]Citrulline was separated by passing reaction mixtures through Dowex AG 50W-X8 ( $\text{Na}^+$  form, Bio-Rad) cation exchange columns and quantitated by liquid scintillation counting[24].

### EPR Spectroscopy and Spin Trapping

Spin-trapping measurements of oxygen free radicals were performed in 50 mM Tris-HCl buffer, pH 7.6, containing 0.5 mM NADPH, 0.5 mM  $\text{Ca}^{2+}$ , 10  $\mu\text{g}/\text{ml}$  calmodulin, 400nM purified eNOS, and 20 mM spin trap DEPMPO. EPR spectra were recorded in a disposable micro-pipette (50 $\mu\text{l}$ , VWR Scientific) at room temperature (23°C) with a Bruker EMX spectrometer

operating at X-band with a high sensitive (HS) cavity (Bruker Instrument, Billerica, MA) using a modulation frequency of 100 kHz, modulation amplitude of 0.5 G, microwave power of 20mW, and microwave frequency of 9.863GHz as described [12, 25]. The central magnetic field was 3510.0 Gauss (G) and the sweep width was 140.0 G. The time constant was 163.84 ms, the sweep rate was 40.96 ms, and the receiver gain was  $2 \times 10^6$ .

## NADPH Consumption by eNOS

NADPH oxidation was measured spectrophotometrically at 340 nm [26]. The reaction systems were the same as described in EPR measurements, and the experiments were run at room temperature. The rate of NADPH oxidation was calculated using a molar extinction coefficient of 6.22 /mM/cm

## Statistics

Data are expressed as means  $\pm$  SE. Comparisons were made using a two-tailed paired or unpaired Student's *t*-test. Differences were considered to be statistically significant at  $P < 0.05$ .

## Results

### Expression of eNOS and Activity Analysis

Both wild type and S1179D eNOS were expressed and purified from *E. Coli*. In a culture of 2 liters, approximately 3.0–4.0 mg of eNOS was typically recovered using 2'5'-ADP Sepharose 4B chromatography. Further purification was performed using FPLC. The final purified products were identified by SDS-PAGE gel (Fig 1A). Previous studies demonstrated that eNOS has higher activity after serine 1179 phosphorylation or Serine 1179 mutation into aspartic acid (S1179D eNOS) [14, 27]. L-citrulline assay demonstrated that WT eNOS can convert L-[14C] arginine to L-[14C] citrulline at a rate of  $2428.6 \pm 420.5$  c.p.m / $\mu$ g protein/min. S1179D eNOS can convert L-[14C] arginine to L-[14C] citrulline at a rate of  $4968.7 \pm 626.6$  c.p.m / $\mu$ g protein/min. Both catalytic activities of WT eNOS and S1179D eNOS were blocked by the NOS inhibitor, L-NAME (1 mM) at  $103.6 \pm 50.2$  and  $217.9 \pm 50.18$  c.p.m/ $\mu$ g protein/min, respectively (Fig 1B).

### BH4 Specifically Inhibited $O_2^{\cdot -}$ Generation from eNOS

Previous studies showed that all three isoforms of NOS, including eNOS generated  $O_2^{\cdot -}$  [8]. To better determine  $O_2^{\cdot -}$  generation from eNOS, we first characterized our DEPMPO and xanthine oxidase/xanthine measurement system. DEPMPO which has a higher affinity for  $O_2^{\cdot -}$  than DMPO and its  $O_2^{\cdot -}$  adduct, DEPMPO-OOH is also more stable than the DMPO- $O_2^{\cdot -}$  adduct [28]. Xanthine oxidase/xanthine (XO/X) is a well-known  $O_2^{\cdot -}$  generation system [29]. A characteristic DEPMPO-OOH adduct signal formed at the range of 3440–3580 Gauss after 20mM DEPMPO was added into a xanthine oxidase/xanthine (XO/X) mixture (Fig 2A left up-trace). To exclude the possibility of BH4 functioning as an  $O_2^{\cdot -}$  scavenger, 100nM BH4 did not affect the DEPMPO-OOH adduct signal generated from XO/X system (Fig 2A left middle-trace), which was consistent with previous observation [30]. Compared to XO/X system, 4 $\mu$ g eNOS generated similar density of DEPMPO-OOH adduct signal in the absence of L-arginine and BH4 (Fig 2A right top trace and Fig 2B). In contrast to DEPMPO-OOH adduct signaling generated from XO/X system, DEPMPO-OOH adduct signaling from eNOS was significantly inhibited by 100nM BH4 (Fig 2A right middle trace and Fig 2B). BH4 did not non-specifically scavenge the  $O_2^{\cdot -}$  until the concentration reached 500nM (data not shown). Moreover, DEPMPO-OOH adduct signals from both the XO/X system and from eNOS were significantly

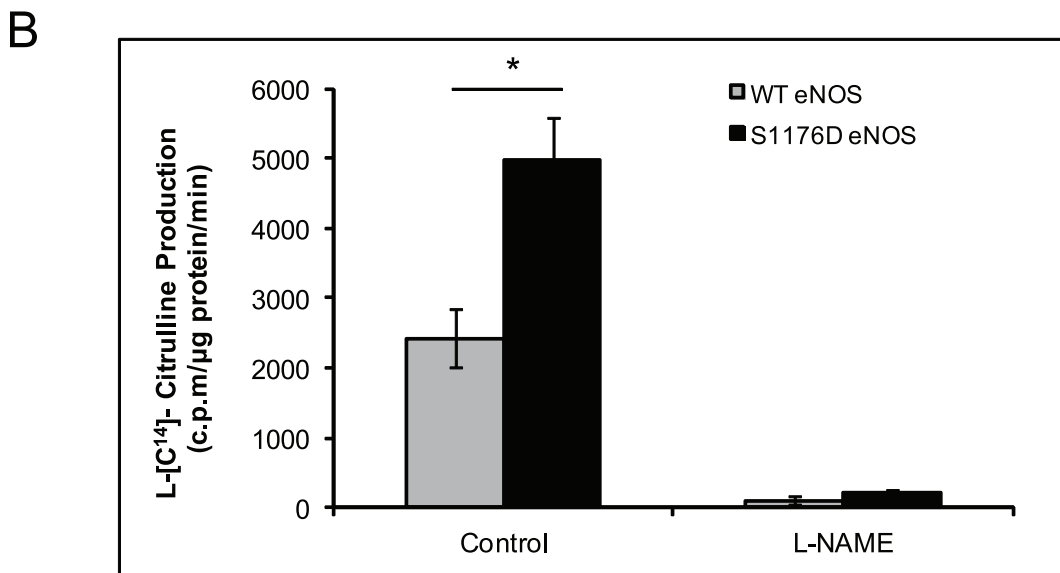
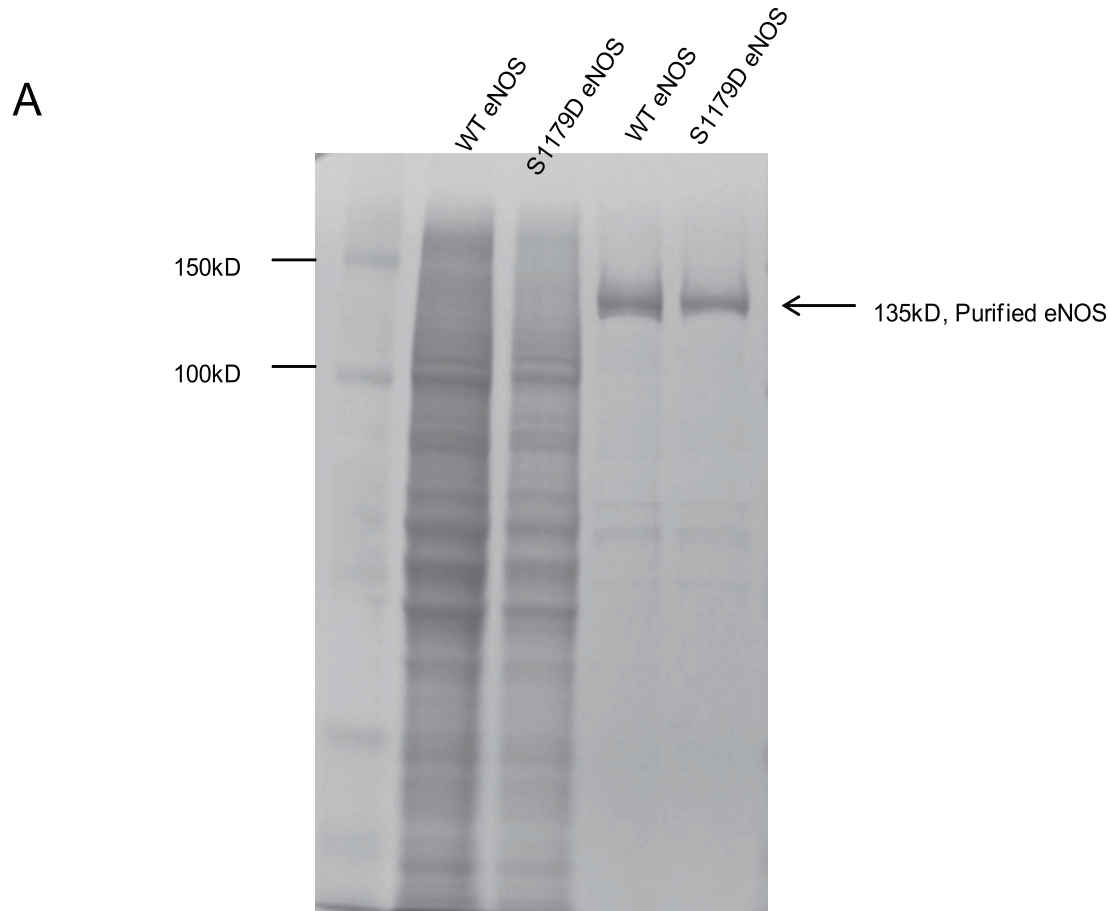


**Fig 1. Mutation of Serine1179 of eNOS enhanced eNOS activity.** (A) The bovine WT eNOS and bovine S1179D eNOS plasmid were expressed in E.Coli. The over-expressed eNOS proteins have been purified by FPLC as indicated in material and methods; the purity of protein was determined by coomassie bright blue stain after 1μg protein were run on SDS-PAGE gel. (B) eNOS activity was assayed by measuring the conversion of L-[<sup>14</sup>C]arginine to L-[<sup>14</sup>C]citrulline. The preparation showed typical eNOS characteristics with L-NAME-inhibitory activity (\*\*, P<0.01; \*, P<0.05 compared with WT eNOS, n = 4).

doi:10.1371/journal.pone.0140365.g001

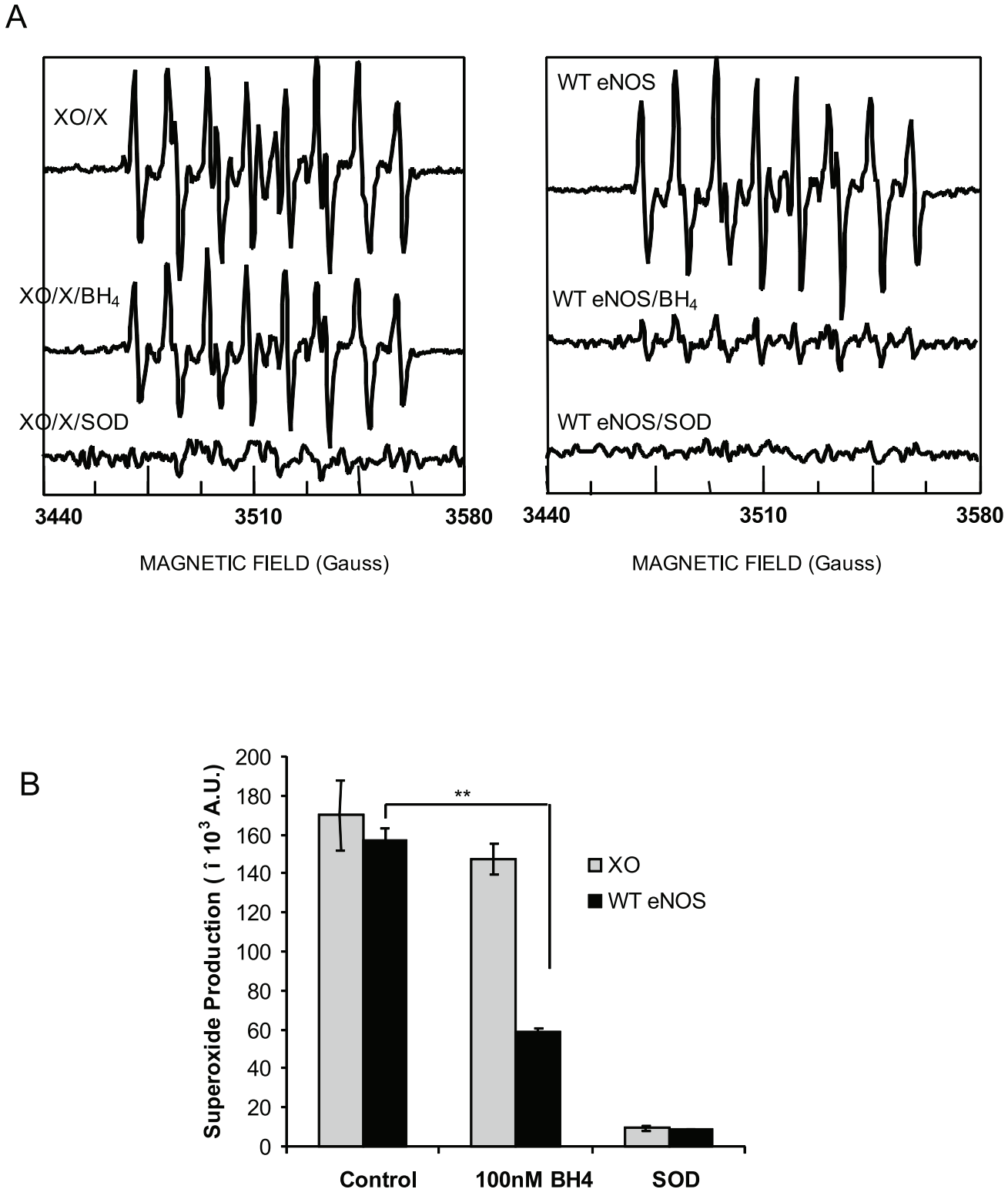


**Fig 2. BH4 specifically inhibited  $O_2^{\cdot -}$  generation from eNOS.** (A) A typical DEPMPPO-OOH adduct signal was detected by a mixture of 0.005U/mL XO and 1mM xanthine, 20mM DEPMPPO in 50mM Tris-HCl buffer, pH 7.6. This DEPMPPO-OOH adduct signal was not inhibited by 100nM BH4. (B) 4 $\mu$ g eNOS protein mixed with 20 mM DEPMPPO in 50 mM Tris-HCl buffer, pH 7.6, containing 0.5 mM NADPH, 0.5 mM  $Ca^{2+}$  (calcium chloride), 10  $\mu$ g/ml calmodulin (CaM). Similar DEPMPPO-OOH adduct signal was recorded by EPR at 3440–3580 Hz range. Different with XO/Xanthine system, DEPMPPO-OOH adduct signal generated from eNOS was significantly but not completely inhibited by 100nM BH4. Both of DEPMPPO-OOH adduct signal generated from XO/Xanthine

system and eNOS were completely inhibited by SOD (200 units/mL). The EPR spectra were representative spectra from five independent experiments and the density was presented as Mean  $\pm$ SD.

doi:10.1371/journal.pone.0140365.g002

abolished by 200 units/mL SOD, indicating that these DEPMPO-OOH adduct signals were products of  $O_2^{\cdot-}$  (Fig 2A bottom traces and Fig 2B).

### BH4 Significantly but Not Completely Inhibited $O_2^{\cdot-}$ Generation from eNOS

BH4 is a critical regulator for  $O_2^{\cdot-}$  generation from eNOS, which binds with oxygenase domain. We next investigated the inhibitory effect of BH4 on  $O_2^{\cdot-}$  generation from eNOS[31]. A prominent DEPMPO-OOH adduct signal was recorded by EPR spectrum when 2 $\mu$ g WT eNOS was incubated with 20mM DEPMPO in the absence of L-arginine and BH4 (Fig 3A second trace). This  $O_2^{\cdot-}$  generation from WT eNOS was significantly inhibited by BH4 in a concentration dependent- manner (from 10nM to 100nM, Fig 3A third to fifth traces). However, BH4 did not completely inhibit  $O_2^{\cdot-}$  generation from WT eNOS even as BH4 concentration increased to 100nM or higher (Fig 3 fifth trace). Considering that BH4 binds with eNOS oxygenase domain, we hypothesized that eNOS may contain another  $O_2^{\cdot-}$  generation site located outside of the eNOS oxygenase domain. BH4 had similar inhibitory effect on  $O_2^{\cdot-}$  generation from S1179D eNOS (Data not shown).

### $O_2^{\cdot-}$ Generated from the eNOS Reductase Domain Was Regulated by Serine 1179 Phosphorylation

Previous NO studies show that eNOS produces NO from a heme center in the oxygenase domain[32]. In addition to L-arginine, eNOS needs NADPH as an electron donor and many other co-factors such as  $Ca^{2+}$ , CaM and BH4 to generating NO. ENOS generates  $O_2^{\cdot-}$  in the absence of L-arginine and BH<sub>4</sub>. In this case the electrons are delivered to heme center and oxygen is oxidized into  $O_2^{\cdot-}$ . In this experiment we first examined whether  $Ca^{2+}$  and CaM affect  $O_2^{\cdot-}$  generation from WT eNOS and S1179D eNOS. EPR spectra showed that there was a strong DEPMPO-OOH adducts signal for WT eNOS. ENOS still generates a significant amount of  $O_2^{\cdot-}$  in the absence of  $Ca^{2+}$  and CaM (38971.5 $\pm$ 2069.9, 34.2 $\pm$ 1.8% compared to that from WT eNOS in presence of  $Ca^{2+}$  /CaM). In  $Ca^{2+}$  and CaM depleted conditions, S1179D eNOS also generated a significant amount of  $O_2^{\cdot-}$  (53186.5 $\pm$ 1520.67, 26.8 $\pm$ 0.7% comparing to S1179D eNOS control. (Fig 4A middle traces). These results indicate that there may be another functional center producing  $O_2^{\cdot-}$  outside of the heme center as the electron was not delivered to heme center. A potential  $O_2^{\cdot-}$  generation site outside oxygenase domain is the FMN and FAD/NADPH center, which locates in the reductase domain of eNOS[11]. As WT eNOS and S1179D eNOS were treated with 10mM DPI, a flavoprotein inhibitor, and the DEPMPO-OOH signals significantly decreased (Fig 4A bottom traces and 4B).

### L-Arginine, BH<sub>4</sub> Did Not Affect the $O_2^{\cdot-}$ Generation from eNOS Reductase Domain

To exclude the potential effect of the oxygenase domain on the  $O_2^{\cdot-}$  release from reductase domain, we used 1mM L-NAME, a heme center inhibitor. L-NAME did not cause a significant inhibitory effect on  $O_2^{\cdot-}$  generation from WT eNOS or S1179D eNOS when compared to control. The DEPMPO-OOH adduct signals from WT eNOS and S1179D eNOS were 37661 $\pm$ 575.2 and 53783  $\pm$  2958.5, respectively. When WT eNOS and S1179D eNOS were treated with L-arginine (1mM), a substrate for NO generation of eNOS which also binds in heme center,

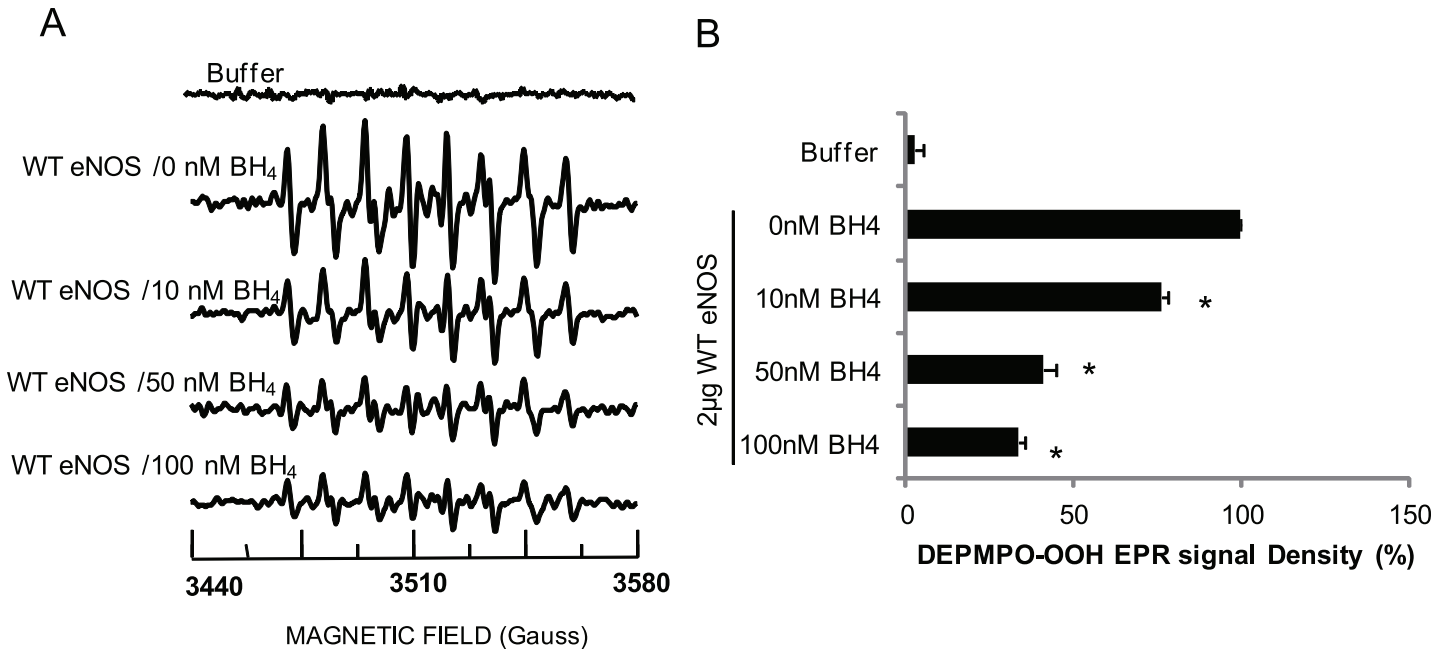


**Fig 3. O<sub>2</sub><sup>-</sup> generated from eNOS was significantly but not completely inhibited by BH<sub>4</sub>.** 2 μg eNOS protein mixed with 20 mM DEPMPPO in 50 mM Tris-HCl buffer, pH 7.6, containing 0.5 mM NADPH, 0.5 mM Ca<sup>2+</sup>, 10 μg/ml CaM and different indicated concentration of BH<sub>4</sub>. (B) Statistical assay showed that DEPMPPO-OOH adduct signals generated from eNOS were significantly inhibited by 10nM BH<sub>4</sub> and decreased as dose-dependently till 100nM BH<sub>4</sub> (n = 4).

doi:10.1371/journal.pone.0140365.g003

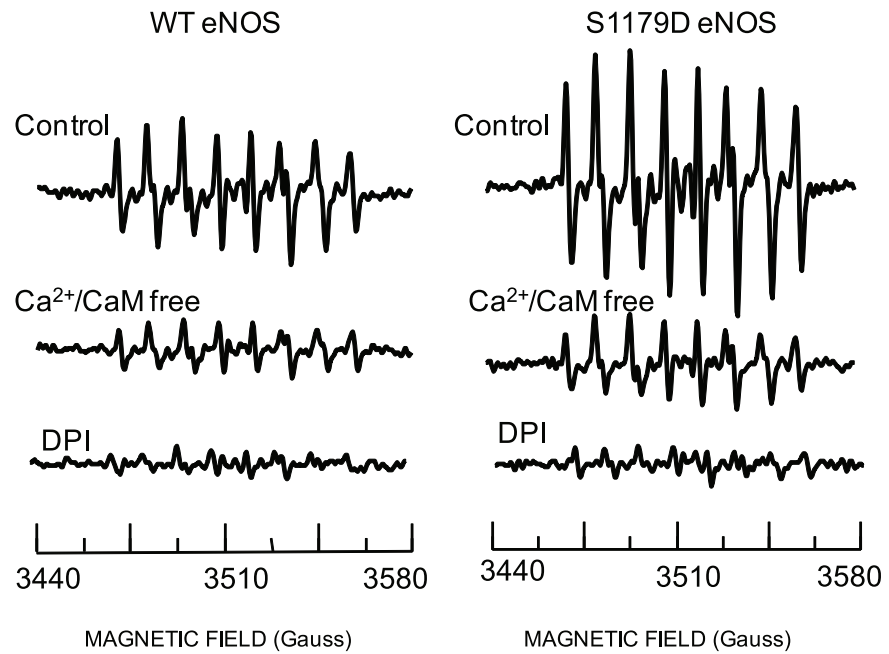
the DEPMPPO-OOH adduct signals generated were 38367±4841.58 and 47520±1533.9 respectively, with no significant difference when compared to controls (Fig 5A).

Early studies showed that BH<sub>4</sub> and L-arginine were the determinant factors regulating NO or O<sub>2</sub><sup>-</sup> generation from eNOS heme center [32–33]. Next we investigated whether BH<sub>4</sub> or BH<sub>4</sub> and L-arginine together affected O<sub>2</sub><sup>-</sup> release from the reductase domain. WT eNOS and S1179D eNOS were incubated BH<sub>4</sub> (100nM) at a Ca<sup>2+</sup>/CaM depletion condition. As shown in Fig 5B, the DEPMPPO-OOH signals generated from WT eNOS and S1179D were 47930.4 ±4679 and 56564.81±5964.4, respectively. When WT eNOS and S1179D eNOS were incubated with BH<sub>4</sub>/ L-arginine (100nM/1mM), the DEPMPPO-OOH signals generated from WT eNOS and S1179D were 41459.65±3403.8 and 54607.8±50.7, respectively (Fig 5B). There was no significant difference between BH<sub>4</sub> treated groups and BH<sub>4</sub>/ L-arginine groups in the absence of Ca<sup>2+</sup> and CaM.

### The Affirmative Evidence of O<sub>2</sub><sup>-</sup> Generation from the eNOS Reductase Domain

To further determine the mechanism of O<sub>2</sub><sup>-</sup> release from the eNOS reductase domain, we sub-cloned the bovine eNOS reductase domain from WT eNOS plasmid and expressed it in E.Coli. 1 μg purified eNOS reductase domain protein was identified on the SDS-page gel (Fig 6A). Compared to WT eNOS without Ca<sup>2+</sup> /CaM, 2 μg purified eNOS reductase domain protein generated an equal amount of O<sub>2</sub><sup>-</sup> (Fig 6B top trace and second trace, respectively). The DEPMPPO-OOH adduct signals were 47392±5090.3 and 49124.05±4332.34, respectively. This O<sub>2</sub><sup>-</sup> generation from eNOS reductase domain was significantly blocked by the FMN/FAD inhibitor, DPI; but not by the heme inhibitor L-NAME (Fig 6B fourth trace and third trace, and Fig 6C).

A



B

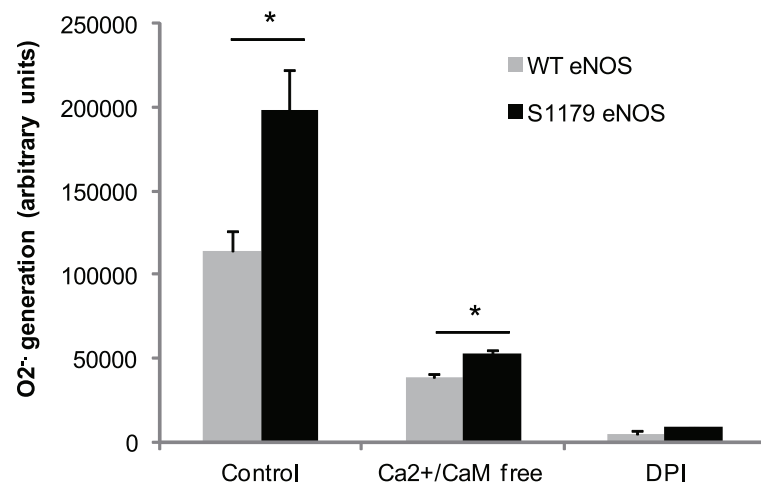


**Fig 4. Ser1179D mutation enhanced both eNOS and reductase domain O<sub>2</sub><sup>-</sup> generation capacity.** 2 μg eNOS protein mixed with 20 mM spin trap DEPMPPO in 50 mM Tris-HCl buffer, pH 7.6 containing 0.5 mM NADPH in presence or absence of 0.5 mM Ca<sup>2+</sup>, 10 μg/ml CaM, the DEPMPPO-OOH adducted were recorded by EPR at 3440 to 3580 Hzs. Data shown are means from three experiments. (A) Wild type eNOS produced a strong DEPMPPO-OOH adduct signal in the Tris HCl buffer in the presence of 0.5 mM Ca<sup>2+</sup>, 10 μg/ml CaM (left up-trace). Compared to wild type eNOS, Ser1179D eNOS have significant higher DEPMPPO-OOH adduct signal (Right up- trace). Depletion of Ca<sup>2+</sup>/CaM with 25mM EDTA significantly decreased O<sub>2</sub><sup>-</sup> generation from WT eNOS (left middle trace) and from S1179D eNOS (right middle trace). Moreover, these DEPMPPO-OOH adduct signals were completely inhibited by 10mM DPI, and FMN/FAD inhibitor (bottom

traces); (B) Statistical analysis indicated that  $O_2^{\cdot-}$  generation from S1179D eNOS was significantly higher than that from WT eNOS ( $P < 0.05$ ,  $n = 5$ ); Depletion of  $Ca^{2+}$ /CaM significantly inhibited  $O_2^{\cdot-}$  generation capacity from both wild type eNOS and S1179D eNOS ( $n = 5$ ,  $P < 0.01$ ).

doi:10.1371/journal.pone.0140365.g004

## NADPH-Consumption Evidence for $O_2^{\cdot-}$ Generation from eNOS Reductase Domain and Regulation by Phosphorylation

As eNOS needs to consume NADPH to generate free electron, NADPH consumption is the indirect index consisting with  $O_2^{\cdot-}$  generation rate. To further exclude other potential  $O_2^{\cdot-}$  generation centers in eNOS, we next compared the NADPH consumption of WT eNOS, S1179D eNOS and purified eNOS reductase domain. At condition of  $Ca^{2+}$  and CaM depletion, there was not significant difference of NADPH consumption rate between WT eNOS and eNOS reductase domain ( $3.49 \pm 0.39 \mu\text{M/h}$  and  $4.03 \pm 0.17 \mu\text{M/h}$  for WT eNOS and eNOS reductase domain respectively,  $P > 0.05$ ). However, S1179D eNOS consumed a significantly higher amount of NADPH than WT eNOS and eNOS reductase domain ( $5.35 \pm 0.58 \mu\text{M/h}$ ,  $P < 0.05$  compare to WT eNOS and reductase domain, respectively. [Fig 7](#)).

## Discussion

In this study, we obtained three important findings. First, spin trapping experiments presented definitive evidence that eNOS generates  $O_2^{\cdot-}$  from the FMN and FAD/NADPH binding site of the reductase domain. Second,  $O_2^{\cdot-}$  generation from eNOS reductase domain is not regulated by eNOS cofactors BH4, L-arginine, and  $Ca^{2+}$ /CaM. However,  $O_2^{\cdot-}$  generation from eNOS reductase domain is regulated by eNOS phosphorylation. Third, purified eNOS reductase domain protein provided direct evidence that the  $O_2^{\cdot-}$  generation center is located in the FMN and FAD/NADPH binding sites of the eNOS reductase domain. Finally, NADPH consumption rate also indicate that eNOS reductase domain has an electron leakage site and generation of  $O_2^{\cdot-}$ .

Although eNOS, nNOS and iNOS have different oxygenase domains and enzyme activities, they have similar structure in their reductase domains those function like NADPH-cytochrome P-450 [13]. Previous studies showed that electron flux leaked from iNOS reductase domain and was not affected by L-arginine [12]. Also, nNOS HSP90 binding studies showed that HSP90 could largely but not completely inhibit  $O_2^{\cdot-}$  generation from nNOS [34–35]. Pharmaceutical inhibitors study showed that nNOS reductase domain may also involve in  $O_2^{\cdot-}$  generation from nNOS [36]. Moreover, a recent study showed that S-glutathionylation of Cysteine 689 and Cysteine 908 in human eNOS increased  $O_2^{\cdot-}$  generation from eNOS. This  $O_2^{\cdot-}$  generation was speculated from eNOS reductase domain as they locate in the FAD/NADPH binding subdomain [11]. In the current study, combining DEPMPO spin trapping with purified eNOS reductase domain protein, we have for the first time offered direct evidence that  $O_2^{\cdot-}$  generated from the FMN and FAD/NADPH binding sites of eNOS. Overall, previous studies and our current study indicated all three isoforms of NOSs generate superoxide from their reductase domain.

As eNOS function is controlled by many factors, including BH4, L-arginine and  $Ca^{2+}$ /CaM, we also investigated the impact of these factors on the function of the eNOS reductase domain. Distinct from  $O_2^{\cdot-}$  generation from the heme center of the eNOS oxygenase domain, BH4, L-arginine and  $Ca^{2+}$ /CaM did not affect  $O_2^{\cdot-}$  generation from eNOS reductase domain. As DPI, a flavoprotein inhibitor, inhibited  $O_2^{\cdot-}$  generation, the generation site may be the flavin center of the FMN and FAD/NADPH binding subdomains.

Unlike the effect of eNOS cofactors on eNOS reductase domain, eNOS Ser1179 phosphorylation enhances  $O_2^{\cdot-}$  generation from eNOS reductase domain. Our results show that mutation of Ser1179D eNOS significantly increases  $O_2^{\cdot-}$  generation from both eNOS oxygenase domain

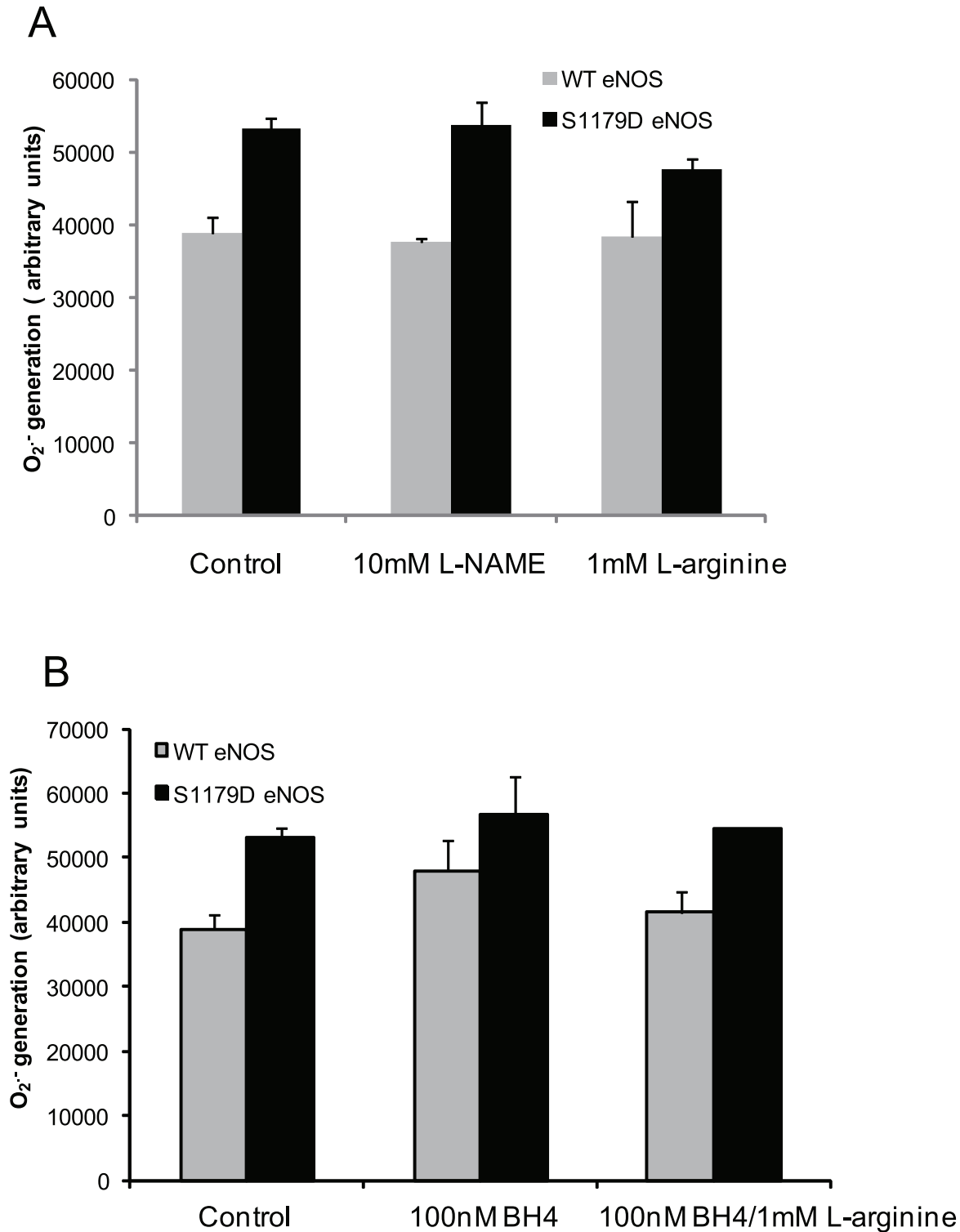


**Fig 5. Both BH<sub>4</sub> and L-arginine do not affect the O<sub>2</sub><sup>-</sup> generation from eNOS in the absence of Ca<sup>2+</sup>/CaM.** After 2µg eNOS protein mixed with 20 mM DEPMPPO in 50 mM Tris-HCl buffer, pH 7.6 containing 0.5 mM NADPH and depletion of Ca<sup>2+</sup>/CaM by adding 20mM EDTA, the DEPMPPO-OOH adduct signal were recorded by EPR at 3440 to 3580 Hzs. (A) At depletion of Ca<sup>2+</sup>/CaM condition, the effect of L-arginine (1 mM) or L-NAME (10mM) on superoxide generation from eNOS. (B) At depletion of Ca<sup>2+</sup>/CaM condition, the effect of BH<sub>4</sub> (100 nM) or BH<sub>4</sub> and L-arginine (1 mM) together on superoxide generation from eNOS. Data shown were the mean values from four independent experiments.

doi:10.1371/journal.pone.0140365.g005

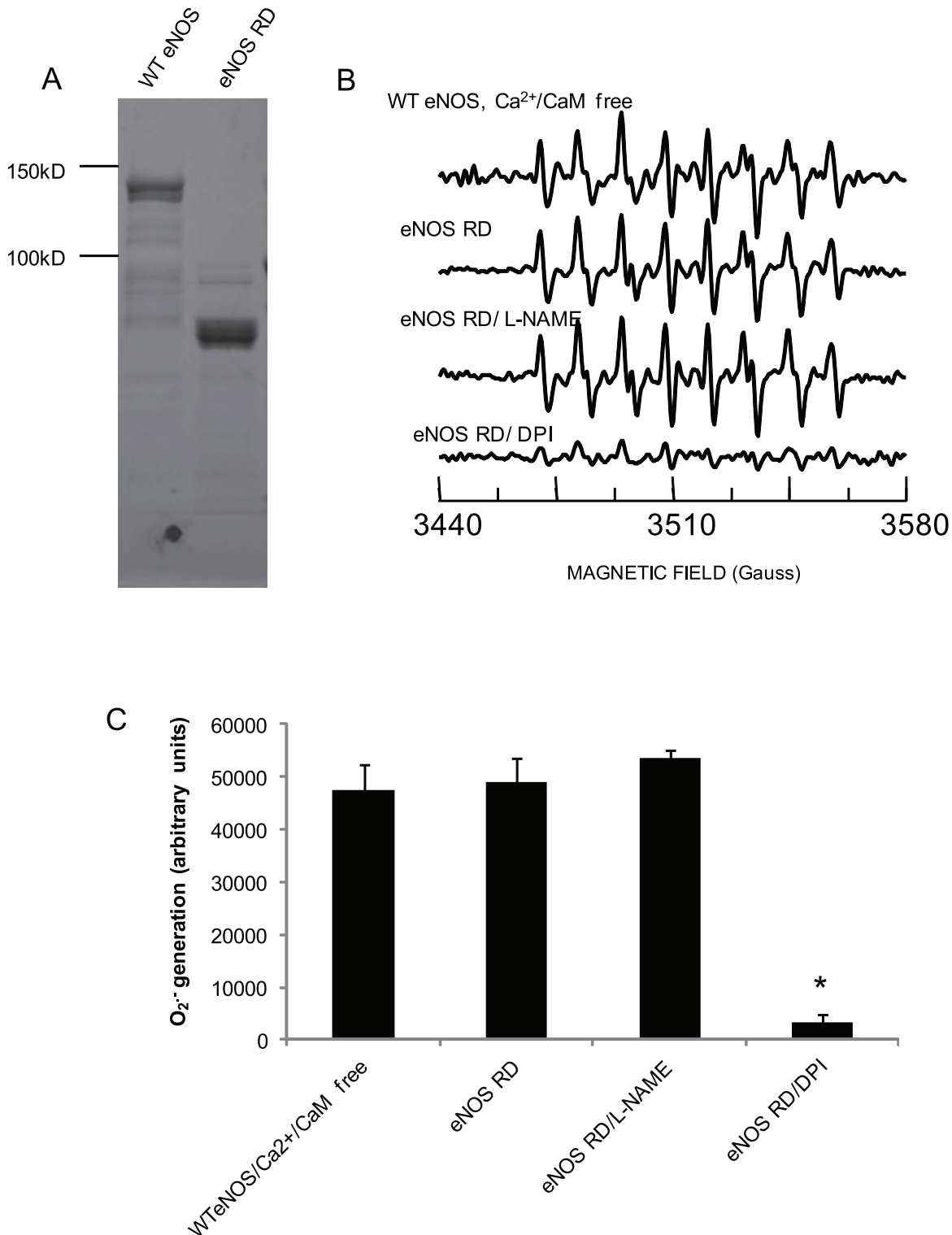


**Fig 6. O<sub>2</sub><sup>-</sup> generates from the cloned eNOS reductase domain.** (A) The recombinant DNA of Bovine eNOS reductase domain was over-expressed in *E. Coli* as described in materials and methods. After purified, the purity was identified on SDS-PAGE gel by Coomassie brilliant blue staining. (B) EPR spectra showed that DEPMPO-OOH adduct signal generated from 2µg purified WT eNOS at condition of Ca<sup>2+</sup>/CaM depletion (*Top trace*); Equal amount of recombinant eNOS reductase domain protein produced equal strong DEPMPO-OOH adduct signal as WT eNOS in the absence of Ca and CaM (*Second trace, RD*); the signal did not inhibited by 10mM L-NAME but inhibited by 10mM DPI (*Third trace and bottom trace*). (C) Statistic analysis confirmed that there

was not significant different of  $O_2^{\cdot-}$  generated from WT eNOS and from recombinant eNOS reductase domain protein and both were inhibited by 10mM DPI. Values are mean  $\pm$  S.E., n = 3–5 determinations.

doi:10.1371/journal.pone.0140365.g006

and eNOS reductase domain (Fig 4). NADPH consumption rates also confirm that eNOS Ser1179 phosphorylation enhances electron generation and electron delivery efficiency, which is indicative of more oxygen molecules converting into  $O_2^{\cdot-}$ . We are on the way to determining the importance of electron redistribution between the eNOS oxygenase domain and eNOS reductase domain caused by eNOS Ser1179 phosphorylation.

Previous observations have found that the eNOS reductase domain binds with NADPH and generates an electron, which is delivered into the heme center of the oxygenase domain[32]. In this study, our results clearly show that FMN and FAD/NADPH binding sites of the eNOS reductase domain also generates  $O_2^{\cdot-}$ . At physiological conditions,  $O_2^{\cdot-}$  generation from the oxygenase domain and reductase domain in WT eNOS are  $65.7 \pm 10.3\%$  and  $34.2 \pm 1.8\%$ , respectively (Figs 2 and 4). Similar NADPH consumption rate by WT eNOS in absence of  $Ca^{2+}/CaM$  and by purified eNOS reductase domain also indicated that the electron was consumed by eNOS reductase domain (Fig 7). Although we did not determine the exact electron leakage site in FMN or FAD/NADPH binding subdomains, our DPI inhibitor results clearly

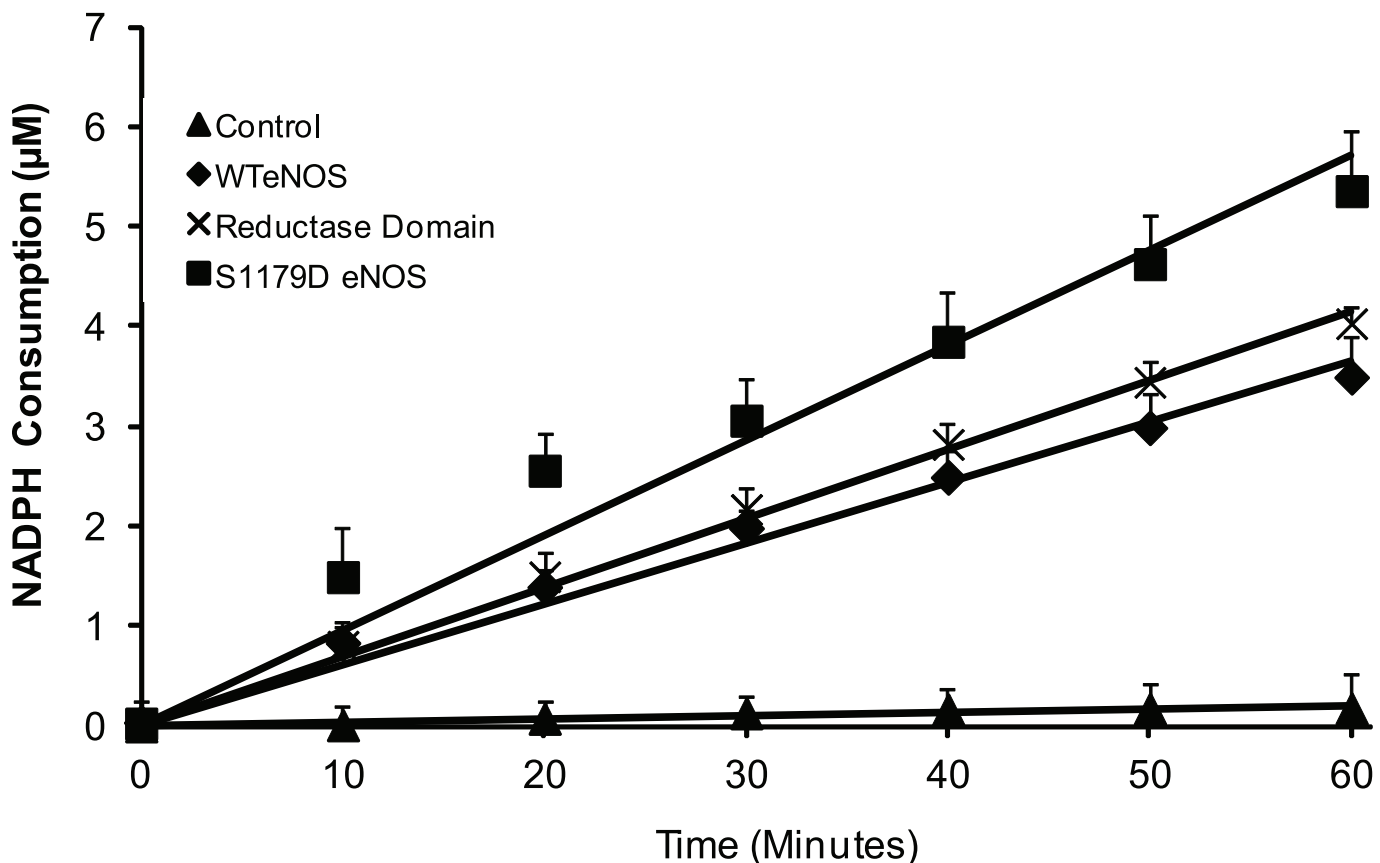


**Fig 7. NADPH consumption by eNOS reductase domain.** NADPH oxidation was monitored spectrophotometrically at 340 nm in the reactions containing 50 mM Tris-HCl, pH 7.4, 60  $\mu$ M NADPH, 32  $\mu$ g/ml eNOS. As shown, self-oxidation of NADPH was 0.3  $\mu$ M per hour in the absence of  $Ca^{2+}/CaM$  (triangle). 2  $\mu$ g WT eNOS and purified recombinant eNOS reductase domain protein consumed 4.5  $\mu$ M NADPH per hour and 4.1  $\mu$ M NADPH per hour in the absence of  $Ca^{2+}/CaM$ , respectively (diamond and cross). However, S1179D eNOS caused 6.3  $\mu$ M NADPH oxidation per hour in the absence of  $Ca^{2+}/CaM$  (rectangle). Data shown are the means of the results from three independent experiments.

doi:10.1371/journal.pone.0140365.g007

indicate the importance of FMN or FAD/NADPH binding sites for eNOS functions. Considering a significant amount of  $O_2^{\cdot-}$  is generated in the eNOS reductase domain (1/3 of total  $O_2^{\cdot-}$  generation from eNOS, Fig 8), it may play critical role in maintenance of eNOS function and dimer structure. While we have identified this new  $O_2^{\cdot-}$  generation center in the eNOS reductase domain, its potential binding cofactor or chaperone protein remain unclear.

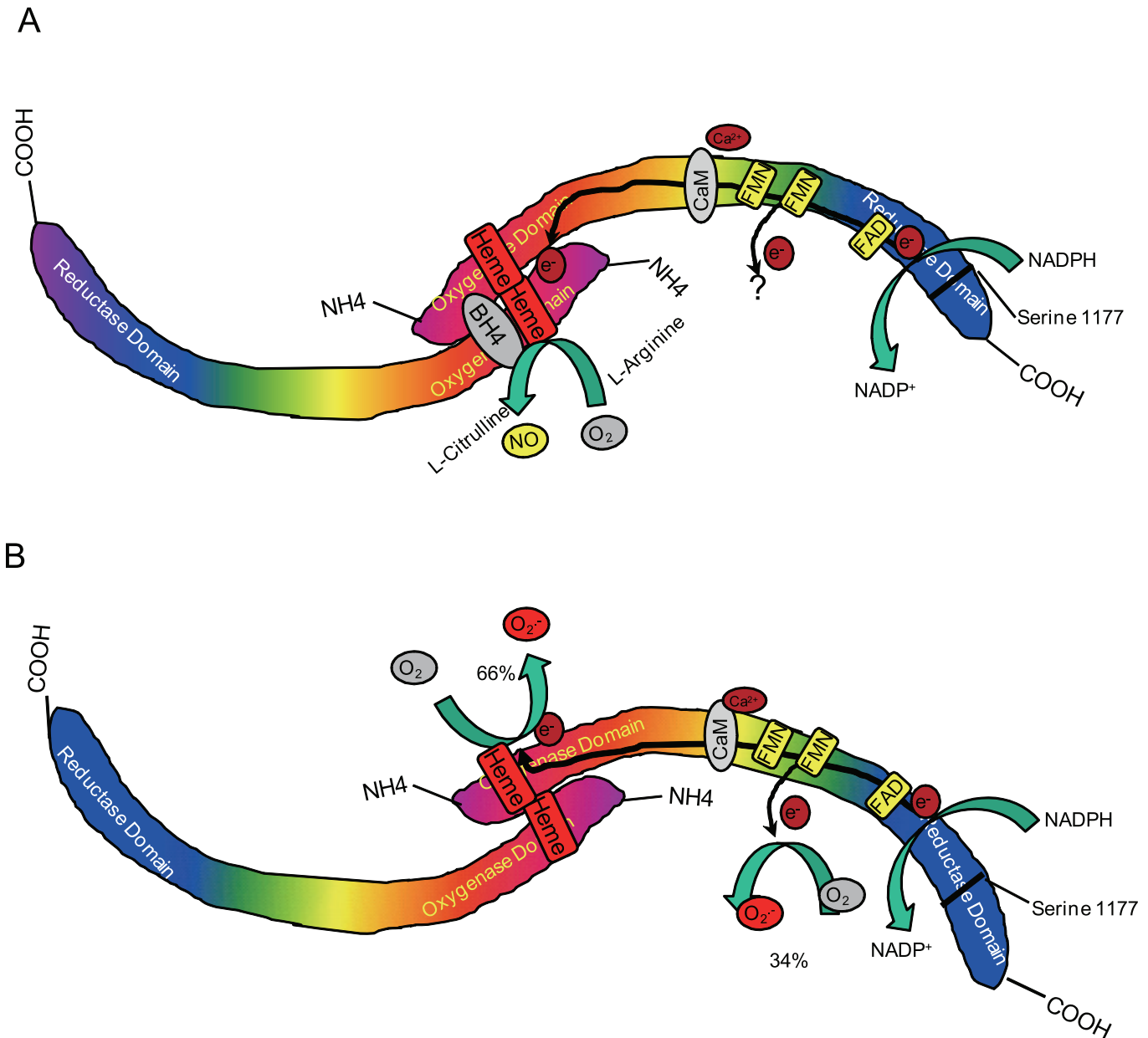


**Fig 8. Schematic diagram illustrating the  $O_2^{\cdot-}$  generation mechanisms from eNOS reductase domain and oxygenase domain.** In addition of heme center of eNOS oxygenase domain (N-terminal),  $O_2^{\cdot-}$  also generates from eNOS reductase domain. This  $O_2^{\cdot-}$  generation center locates in the FMN and FAD/NADPH binding site. (A) At BH4 and L-arginine binding condition, electron generated from eNOS reductase domain is delivered into heme center of another eNOS oxygenase domain and generates NO. By binding with FMN or FAD, electron leakage in FMN and FAD/NADPH binding site is also inhibited; (B) However, at uncouple condition (BH4 and L-arginine depletion), the electron generated from eNOS reductase domain is delivered into same eNOS oxygenase domain and generates  $O_2^{\cdot-}$ . Moreover, the electron leakage at FMN and FAD/NADPH binding sites also results in  $O_2^{\cdot-}$  generation. The  $O_2^{\cdot-}$  generation capacity in heme center of oxygenase domain and flavin center of reductase domain are 65.8% and 34.2% respectively.

doi:10.1371/journal.pone.0140365.g008

## Conclusion

In conclusion, we offer direct evidence to identify a new  $O_2^-$  generation site in the eNOS reductase domain. This site is not regulated by BH<sub>4</sub>, L-arginine and Ca<sup>2+</sup>/CaM, but it is enhanced by eNOS phosphorylation. The  $O_2^-$  generation capacity of the eNOS reductase domain is around 1/3 of the total eNOS  $O_2^-$  generation capacity. Studies with pharmacologic inhibitors and cloned eNOS constructs indicate that this  $O_2^-$  generation site is located in the FMN and FAD/NADPH binding region of eNOS reductase domain. These novel findings will aid the understanding of eNOS function and may help in the development of new therapeutic strategy for the patients suffering eNOS dysfunction related diseases.

## Acknowledgments

Special thanks to Dr. Mark C Harbeck for English correction and discussion.

## Author Contributions

Conceived and designed the experiments: HP WC YZ. Performed the experiments: HP YC YZ. Analyzed the data: AR WC. Contributed reagents/materials/analysis tools: WC HP YZ. Wrote the paper: HP AR WC.

## References

1. Shesely EG, Maeda N, Kim HS, Desai KM, Krege JH, Laubach VE, et al. Elevated blood pressures in mice lacking endothelial nitric oxide synthase. *Proc Natl Acad Sci U S A*. 1996; 93(23):13176–81. PMID: [8917564](#).
2. Huang PL, Huang Z, Mashimo H, Bloch KD, Moskowitz MA, Bevan JA, et al. Hypertension in mice lacking the gene for endothelial nitric oxide synthase. *Nature*. 1995; 377(6546):239–42. PMID: [7545787](#).
3. Sessa WC, Garcia-Cardena G, Liu J, Keh A, Pollock JS, Bradley J, et al. The Golgi association of endothelial nitric oxide synthase is necessary for the efficient synthesis of nitric oxide. *J Biol Chem*. 1995; 270(30):17641–4. PMID: [7543089](#).
4. Wu KK. Regulation of endothelial nitric oxide synthase activity and gene expression. *Ann N Y Acad Sci*. 2002; 962:122–30. PMID: [12076969](#).
5. Xia Y, Dawson VL, Dawson TM, Snyder SH, Zweier JL. Nitric oxide synthase generates superoxide and nitric oxide in arginine-depleted cells leading to peroxynitrite-mediated cellular injury. *Proc Natl Acad Sci U S A*. 1996; 93(13):6770–4. PMID: [8692893](#).
6. Berka V, Wang LH, Tsai AL. Oxygen-induced radical intermediates in the nNOS oxygenase domain regulated by L-arginine, tetrahydrobiopterin, and thiol. *Biochemistry*. 2008; 47(1):405–20. PMID: [18052254](#).
7. Berka V, Wu G, Yeh HC, Palmer G, Tsai AL. Three different oxygen-induced radical species in endothelial nitric-oxide synthase oxygenase domain under regulation by L-arginine and tetrahydrobiopterin. *The Journal of biological chemistry*. 2004; 279(31):32243–51. PMID: [15166218](#).
8. Xia Y, Tsai AL, Berka V, Zweier JL. Superoxide generation from endothelial nitric-oxide synthase. A Ca<sup>2+</sup>/calmodulin-dependent and tetrahydrobiopterin regulatory process. *J Biol Chem*. 1998; 273(40):25804–8. PMID: [9748253](#).
9. Lamas S, Marsden PA, Li GK, Tempst P, Michel T. Endothelial nitric oxide synthase: molecular cloning and characterization of a distinct constitutive enzyme isoform. *Proc Natl Acad Sci U S A*. 1992; 89(14):6348–52. Epub 1992/07/15. PMID: [1378626](#); PubMed Central PMCID: PMC49498.
10. Goligorsky MS. Endothelial nitric oxide synthase: from structure to function in one aspartic substitution. *Kidney Int*. 2009; 75(3):255–7. Epub 2009/01/17. doi: [10.1038/ki.2008.605](#) [pii] doi: [10.1038/ki.2008.605](#) PMID: [19148150](#).
11. Chen CA, Wang TY, Varadharaj S, Reyes LA, Hemann C, Talukder MA, et al. S-glutathionylation uncouples eNOS and regulates its cellular and vascular function. *Nature*. 2010; 468(7327):1115–8. Epub 2010/12/24. doi: [nature09599](#) [pii] doi: [10.1038/nature09599](#) PMID: [21179168](#); PubMed Central PMCID: PMC3370391.
12. Xia Y, Roman LJ, Masters BS, Zweier JL. Inducible nitric-oxide synthase generates superoxide from the reductase domain. *J Biol Chem*. 1998; 273(35):22635–9. PMID: [9712892](#).

13. Alderton WK, Cooper CE, Knowles RG. Nitric oxide synthases: structure, function and inhibition. *The Biochemical journal*. 2001; 357(Pt 3):593–615. Epub 2001/07/21. PMID: [11463332](#); PubMed Central PMCID: PMC1221991.
14. Fulton D, Gratton JP, McCabe TJ, Fontana J, Fujio Y, Walsh K, et al. Regulation of endothelium-derived nitric oxide production by the protein kinase Akt. *Nature*. 1999; 399(6736):597–601. PMID: [10376602](#).
15. Dimmeler S, Fleming I, Fisslthaler B, Hermann C, Busse R, Zeiher AM. Activation of nitric oxide synthase in endothelial cells by Akt-dependent phosphorylation. *Nature*. 1999; 399(6736):601–5. PMID: [10376603](#).
16. McCabe TJ, Fulton D, Roman LJ, Sessa WC. Enhanced electron flux and reduced calmodulin dissociation may explain "calcium-independent" eNOS activation by phosphorylation. *J Biol Chem*. 2000; 275(9):6123–8. PMID: [10692402](#).
17. Whitsett J, Martasek P, Zhao H, Schauer DW, Hatakeyama K, Kalyanaraman B, et al. Endothelial cell superoxide anion radical generation is not dependent on endothelial nitric oxide synthase-serine 1179 phosphorylation and endothelial nitric oxide synthase dimer/monomer distribution. *Free radical biology & medicine*. 2006; 40(11):2056–68. Epub 2006/05/24. doi: S0891-5849(06)00092-X [pii] doi: [10.1016/j.freeradbiomed.2006.02.001](#) PMID: [16716906](#).
18. Shi Y, Baker JE, Zhang C, Tweddell JS, Su J, Pritchard KA Jr. Chronic hypoxia increases endothelial nitric oxide synthase generation of nitric oxide by increasing heat shock protein 90 association and serine phosphorylation. *Circulation research*. 2002; 91(4):300–6. Epub 2002/08/24. PMID: [12193462](#).
19. Maia AR, Batista TM, Victorio JA, Clerici SP, Delbin MA, Carneiro EM, et al. Taurine supplementation reduces blood pressure and prevents endothelial dysfunction and oxidative stress in post-weaning protein-restricted rats. *PLoS One*. 014; 9(8):e105851. Epub 2014/08/30. doi: [10.1371/journal.pone.0105851](#) PONE-D-14-11309 [pii]. PMID: [25170895](#); PubMed Central PMCID: PMC4149434.
20. Cortes-Gonzalez C, Barrera-Chimal J, Ibarra-Sanchez M, Gilbert M, Gamba G, Zentella A, et al. Opposite effect of Hsp90alpha and Hsp90beta on eNOS ability to produce nitric oxide or superoxide anion in human embryonic kidney cells. *Cell Physiol Biochem*. 2010; 26(4–5):657–68. Epub 2010/11/11. doi: 000322333 [pii] doi: [10.1159/000322333](#) PMID: [21063103](#).
21. Chen CA, Druhan LJ, Varadharaj S, Chen YR, Zweier JL. Phosphorylation of endothelial nitric-oxide synthase regulates superoxide generation from the enzyme. *The Journal of biological chemistry*. 2008; 283(40):27038–47. PMID: [18622039](#). doi: [10.1074/jbc.M802269200](#)
22. Du M, Yeh HC, Berka V, Wang LH, Tsai AL. Redox properties of human endothelial nitric-oxide synthase oxygenase and reductase domains purified from yeast expression system. *The Journal of biological chemistry*. 2003; 278(8):6002–11. PMID: [12480940](#).
23. Martasek P, Liu Q, Liu J, Roman LJ, Gross SS, Sessa WC, et al. Characterization of bovine endothelial nitric oxide synthase expressed in *E. coli*. *Biochem Biophys Res Commun*. 1996; 219(2):359–65. Epub 1996/02/15. doi: S0006-291X(96)90238-7 [pii] doi: [10.1006/bbrc.1996.0238](#) PMID: [8604992](#).
24. Giraldez RR, Panda A, Xia Y, Sanders SP, Zweier JL. Decreased nitric-oxide synthase activity causes impaired endothelium-dependent relaxation in the posts ischemic heart. *The Journal of biological chemistry*. 1997; 272(34):21420–6. PMID: [9261157](#).
25. Song Y, Cardounel AJ, Zweier JL, Xia Y. Inhibition of superoxide generation from neuronal nitric oxide synthase by heat shock protein 90: implications in NOS regulation. *Biochemistry*. 2002; 41(34):10616–22. PMID: [12186546](#).
26. Vasquez-Vivar J, Martasek P, Hogg N, Masters BS, Pritchard KA Jr., Kalyanaraman B. Endothelial nitric oxide synthase-dependent superoxide generation from adriamycin. *Biochemistry*. 1997; 36(38):11293–7. PMID: [9333325](#).
27. Fulton D, Fontana J, Sowa G, Gratton JP, Lin M, Li KX, et al. Localization of endothelial nitric-oxide synthase phosphorylated on serine 1179 and nitric oxide in Golgi and plasma membrane defines the existence of two pools of active enzyme. *The Journal of biological chemistry*. 2002; 277(6):4277–84. Epub 2001/12/01. doi: [10.1074/jbc.M106302200](#) M106302200 [pii] PMID: [11729179](#).
28. Liu KJ, Miyake M, Panz T, Swartz H. Evaluation of DEPMPO as a spin trapping agent in biological systems. *Free radical biology & medicine*. 1999; 26(5–6):714–21. Epub 1999/04/28. doi: S0891-5849(98)00251-2 [pii]. PMID: [10218661](#).
29. Jia ZQ, Zhu H, Misra BR, Mahaney JE, Li YB, Misra HP. EPR studies on the superoxide-scavenging capacity of the nutraceutical resveratrol. *Mol Cell Biochem*. 2008; 313(1–2):187–94. doi: [10.1007/s11010-008-9756-y](#) ISI:000256091000021. PMID: [18409032](#)
30. Vasquez-Vivar J, Whitsett J, Martasek P, Hogg N, Kalyanaraman B. Reaction of tetrahydrobiopterin with superoxide: EPR-kinetic analysis and characterization of the pteridine radical. *Free Radic Biol Med*. 2001; 31(8):975–85. Epub 2001/10/12. doi: S0891584901006803 [pii]. PMID: [11595382](#).

31. Vasquez-Vivar J, Kalyanaraman B, Martasek P, Hogg N, Masters BS, Karoui H, et al. Superoxide generation by endothelial nitric oxide synthase: the influence of cofactors. *Proceedings of the National Academy of Sciences of the United States of America*. 1998; 95(16):9220–5. PMID: [9689061](#).
32. Andrew PJ, Mayer B. Enzymatic function of nitric oxide synthases. *Cardiovasc Res*. 1999; 43(3):521–31. PMID: [10690324](#).
33. Chen W, Druhan LJ, Chen CA, Hemann C, Chen YR, Berka V, et al. Peroxynitrite induces destruction of the tetrahydrobiopterin and heme in endothelial nitric oxide synthase: transition from reversible to irreversible enzyme inhibition. *Biochemistry*. 2010; 49(14):3129–37. PMID: [20184376](#). doi: [10.1021/bi9016632](#)
34. Song Y, Zweier JL, Xia Y. Determination of the enhancing action of HSP90 on neuronal nitric oxide synthase by EPR spectroscopy. *Am J Physiol Cell Physiol*. 2001; 281(6):C1819–24. PMID: [11698240](#).
35. Garcia-Cardena G, Fan R, Shah V, Sorrentino R, Cirino G, Papapetropoulos A, et al. Dynamic activation of endothelial nitric oxide synthase by Hsp90. *Nature*. 1998; 392(6678):821–4. PMID: [9580552](#).
36. Miller RT, Martasek P, Roman LJ, Nishimura JS, Masters BS. Involvement of the reductase domain of neuronal nitric oxide synthase in superoxide anion production. *Biochemistry*. 1997; 36(49):15277–84. Epub 1998/01/10. doi: [10.1021/bi972022c](#) bi972022c [pii] PMID: [9398256](#).